Schema representations in distinct brain networks support narrative memory during encoding and retrieval

Rolando Masís-Obando[1*], **Kenneth A. Norman**[1,2], **Christopher Baldassano**[3]

*For correspondence:
rmasis@princeton.edu (RMO)

[1]Princeton Neuroscience Institute, Princeton, NJ, USA; [2]Department of Psychology, Princeton University, Princeton, NJ, USA; [3]Department of Psychology, Columbia University, New York, NY, USA

Abstract   Schematic prior knowledge can scaffold the construction of event memories during perception and also provide structured cues to guide memory search during retrieval. We measured the activation of story-specific and schematic representations using fMRI while participants were presented with 16 stories and then recalled each of the narratives, and related these activations to memory for specific story details. We predicted that schema representations in mPFC would be correlated with successful recall of story details. In keeping with this prediction, an anterior mPFC region showed a significant correlation between activation of schema representations at encoding and subsequent behavioral recall performance; however, this mPFC region was not implicated in schema representation during retrieval. More generally, our analyses revealed largely distinct brain networks at encoding and retrieval in which schema activation was related to successful recall. These results provide new insight into when and where event knowledge can support narrative memory.

Introduction

How do we remember real-world events? Over the past half-century, the cognitive psychology literature has shown that we leverage event schemas – our knowledge of how events generally unfold – to support memory for specific details from those events (for reviews of early work see *Graesser and Nakamura, 1982*; *Alba and Hasher, 1983*; *Brewer and Nakamura, 1984*; and for more recent cognitive neuroscience studies see *van Kesteren et al., 2012*; *Ghosh and Gilboa, 2014*; *Schlichting and Preston, 2015*; *Gilboa and Marlatte, 2017*; *Preston and Eichenbaum, 2013*; *Wang and Morris, 2010*). For example, when we go into a restaurant, we can anticipate a stereotyped sequence of events that includes getting seated, ordering food, and eating (*Bower et al., 1979*). The cognitive psychology literature has demonstrated that knowledge of this "restaurant script" can help memory in at least two possible ways: At encoding, the restaurant script can provide a scaffold onto which we can attach specific event details (e.g., *Bransford and Johnson, 1972*; *Alba and Hasher, 1983*; *Abbott et al., 1985*; *Tompary and Thompson-Schill, 2021*; *McClelland et al., 2020*); later, at retrieval, the restaurant script provides a structured way of cueing memory, by stepping through the various stages of the script in sequence (e.g., *Schank and Abelson, 1975*; *Anderson and Pichert, 1978*; *Bower et al., 1979*; *Alba and Hasher, 1983*; *Mandler, 2014*).

The goal of the present study is to understand the neural mechanisms of how event schemas

support memory for real-world, temporally-extended events, both at encoding and at retrieval. To meet this objective, we track schema representations in the brain during both encoding and re-trieval of temporally-extended events, and then relate these neural measures to behavioral recall on a story-by-story basis. While there has been an explosion of recent neuroscientific research into how schemas benefit memory (*Maguire et al., 1999*; *van Kesteren et al., 2010a, 2013, 2018, 2020*; *Spalding et al., 2015*; *Liu et al., 2018*; *Brod et al., 2015*; *Brod and Shing, 2018*; *van Buuren et al., 2014*; *Wagner et al., 2015*; *Bein et al., 2014*; *Schlichting and Preston, 2016*; *Tse et al., 2007, 2011*; *Webb et al., 2016*; *Gilboa and Marlatte, 2017*; *Raykov et al., 2021*; *Reagh et al., 2021*), most of this research has relied on univariate contrasts of brain activations evoked by schema-consistent vs. schema-inconsistent learning materials, rather than trying to track the degree to which schematic information is represented for individual stimuli. Also, existing studies have mostly looked at rela-tively simple forms of schematic knowledge (e.g. seashells at the beach vs lamps at a playground; *McAndrews et al., 2016*) rather than knowledge about the structure of real-world, temporally-extended events. Lastly, because existing paradigms have mostly tested memory with recogni-tion or short associative recall tasks, the neural mechanisms of how schemas are instantiated and maintained during free recall of real-world events have not been thoroughly explored.

The present study builds on our prior work (*Baldassano et al., 2018*), in which participants were scanned as they watched movies or listened to audio narratives, half of which followed a restaurant script and half of which followed an airport script. A key benefit of this paradigm is that it allowed us to identify sequences of neural patterns that are unique to particular stories (e.g., sequences of patterns that are reliably invoked by a particular airport narrative, more so than by other air-port narratives) and sequences of patterns that represent the underlying script (e.g., sequences of patterns that are shared across different airport narratives, more so than across restaurant and airport narratives). *Baldassano et al.* (*2018*) leveraged this to identify a range of areas that repre-sented schematic information (i.e., restaurant vs. airport) in a modality-independent fashion. Of the ROIs investigated, medial prefrontal cortex (mPFC) was the only one that was sensitive to the specific temporal order of events in a schema. Here, we extend the *Baldassano et al.* (*2018*) results by analyzing neural and behavioral data from a separate phase of the experiment (not reported in the 2018 study) in which participants were scanned while freely recalling each of the 16 narratives. This allowed us to look at how schemas are represented in the brain during recall, and how neural measures of schema representation at encoding and recall are related to recall of specific story details, on a story-by-story basis.

Because mPFC has been frequently implicated in previous schema research (e.g., *van Kesteren et al., 2010a, 2013, 2014, 2020*; *Baldassano et al., 2018*; *Raykov et al., 2020, 2021*; *Reagh et al., 2021*) – in particular with regard to integrating new knowledge into existing schemas (*Preston and Eichen-baum, 2013*; *Schlichting and Preston, 2015*; *Gilboa and Marlatte, 2017*; *Tse et al., 2007*; *Wang and Morris, 2010*; *van Kesteren et al., 2012*) – we predicted that robust mPFC schema representations at encoding would lead to improved subsequent memory for the narrative. Based on prior work im-plicating the hippocampus in schema representation (*van Kesteren et al., 2013, 2014, 2020*; *Brod et al., 2015*; *Liu et al., 2017*; *Raykov et al., 2020*; *Webb et al., 2016*; *van der Linden et al., 2017*; *Bonasia et al., 2018*), we also hypothesized that hippocampal schema representations at encoding would support subsequent memory; more specifically, based on work showing that hippocampus has a coarse-to-fine gradient of representations along its long axis (*Collin et al., 2015*; *Guo and Yang, 2020*; *Audrain and McAndrews, 2020*; *Poppenk et al., 2013*; *Brunec et al., 2018*; *Schlichting et al., 2015*; *Sekeres et al., 2018*), we predicted that anterior hippocampus (which has coarser and thus more general representations than posterior hippocampus) would contain schematic representa-tions that contribute to subsequent memory, whereas posterior hippocampus would contribute to subsequent memory by representing story-specific details.

As described below, our prediction about mPFC was upheld: An anterior region of mPFC was among the network of cortical regions – also including left visual cortex, right lateral superior frontal gyrus (SFG), prostriata, and entorhinal cortex – where the degree of schema representation at

91 encoding predicted subsequent memory for story details. Our prediction about hippocampus re-
92 ceived partial support: While the degree of schema representation in anterior hippocampus during
93 encoding showed a nonsignificant, positive numerical relationship to subsequent memory for story
94 details, posterior hippocampus showed a negative correlation between schema representation at
95 encoding and subsequent memory, and a positive correlation between the representation of story-
96 specific details at encoding and subsequent memory – both of which are consistent with a role for
97 posterior hippocampus in encoding story-specific (i.e., non-schematic) information. Interestingly,
98 the set of regions where schema representation at encoding predicted recall of story details was
99 mostly distinct from the set of regions where schema representation at retrieval predicted recall of
100 story details – the latter analysis revealed a distinct network including bilateral visual cortex, right
101 superior parietal lobule (SPL), bilateral middle frontal gyrus (MFG), bilateral medial SFG, bilateral
102 parahippocampal cortex (PHC), left fusiform gyrus, right angular gyrus (AG), as well as bilateral
103 posterior superior temporal sulcus, but notably *excluding* mPFC. This pattern of results provides
104 converging neural support for the idea that schemas play different roles at encoding and retrieval
105 in supporting memory for story details.

Results

107 Our primary goal was to understand how we use schemas at encoding and recall to support mem-
108 ory for recently encoded naturalistic stories. To do this we used 16 narratives that conformed
109 to one of two schematic scripts (*Bower et al., 1979*): eating at a restaurant or catching a flight at
110 an airport (**Fig 1**). Each narrative followed a four-event temporal structure specific to its schema
111 (*restaurant stories*: entering the restaurant, being seated, ordering and eating food; *airport stories*:
112 entering the airport, going through security, boarding at gate, and getting seated on plane). During
113 the encoding phase, participants were scanned while they watched or listened to each of these 3
114 minute narratives. Afterwards, during the recall phase, participants were cued with the titles of
115 each of the stories, and were asked to freely verbally recall one story at a time.

Figure 1. Methods. (A.) Stimuli. There were a total of 16 narratives (audiovisual clips or spoken narration): eight restaurant narratives and eight airport narratives. Each narrative followed a four-event temporal structure specific to its schema (see text). **(B.)** Experimental protocol. After *Figure 1 continued on next page.*

Figure 1 continued.

participants encoded each of the narratives, they were then asked to freely recall each of them with a title cue only. **(C.)** Encoding story and schema score. For each story in each participant, a spatial activity pattern was extracted for each of the four events in that story. We then computed, for each participant, the 16 x 16 neural similarity matrix correlating the neural representations of each of the 16 stories in that participant and the neural representations of each of the 16 stories, averaged across the other participants (see text for details). For each story in each participant, we computed an *encoding story score* contrasting across-subject neural similarity to the same story (dark pink) vs. different stories from the same schema (light pink); we also computed an *encoding schema score* contrasting across-subject neural similarity to different stories from the same schema (dark blue) vs. different stories from the other schema (light blue). **(D.)** Reinstatement story and schema score. We used Hidden Markov Models (HMMs) to measure the degree to which each of the 16 stories from the encoding phase was neurally reinstated during recall of a given story (see text for details). This process yielded a 16 story x 16 story neural reinstatement matrix for each participant. Analogously to **C**, for each recall we computed a *reinstatement story score* (contrasting how well the same story's encoding pattern was reinstated vs. other stories from the same schema) and a *reinstatement schema score* (contrasting how well other stories from the same schema were reinstated vs. other stories from the other schema). **(E.)** Behavioral memory performance. Every participant's free recall was scored using a rubric to measure the number of story-specific details the participant provided. This matrix has been sorted such that the most accurate recalls are in the bottom-left. Red and blue story labels indicate restaurant vs airport narratives, respectively. **(F.)** Predicting behavioral memory performance. We used the 4 scores derived from **C** and **D** (encoding story/schema and reinstatement story/schema) in 4 separate regression models to predict behavioral memory performance in **E**.

Neural story and schema scores

Encoding scores

We derived two types of neural scores that reflected the extent to which story-specific and general schematic information were represented during encoding (**Fig 1C**). These scores were computed in both searchlights and specific ROIs (cortical ROIs: mPFC, posterior medial cortex (PMC), AG, PHC, and SFG; hippocampal ROIs: full hippocampus, anterior hippocampus, and posterior hippocampus). Within each story, we computed the mean spatial pattern evoked during each of the four events for each participant. Then, for each pair of stories (call them story A and story B), we applied leave-one-participant-out spatial intersubject correlation, correlating the four story A event patterns from the left-out participant with the four story B event patterns from the other participants. As in *Baldassano et al.* (*2018*), this correlation was computed in an event-wise fashion (correlating event 1 in story A with event 1 in story B, event 2 in story A with event 2 in story B, and so on) and then the four event-wise correlations were averaged together to obtain a single correlation score for the pair of stories. To measure the degree of story-specific representation at encoding for a participant experiencing a particular story, we computed an *encoding story score*, operationalized as the across-participant similarity to the representation of the *same* story, minus the average across-participant similarity to other stories from the same schema. To measure the degree of schematic representation at encoding, we computed an *encoding schema score*, operationalized as the average across-participant similarity to other stories from the same schema, minus the average across-participant similarity to other stories from the other schema. For all analyses reported below on our specific *a priori* ROIs, we report multiple comparisons Bonferroni-corrected p-values, such that p-values for cortical ROIs (n=5) and hippocampal ROIs (n=3) were scaled by 5 or 3, respectively, to uphold a significance level of alpha = 0.05.

Results from this encoding analysis were previously reported in *Baldassano et al.* (*2018*) using a similar analysis pipeline. Encoding story scores were high across all of cortex (**Fig 2A**; q < 0.05), including all of our cortical and hippocampal ROIs (all p < 0.01), with the strongest effects in posterior sensory regions. Strong encoding schema scores were obtained throughout the default mode network (**Fig 2B**; p<0.01 for all cortical ROIs). Additionally, there were strong schematic patterns in anterior but not posterior hippocampus (p<0.01 for whole hippocampus and anterior hippocampus; p=0.27 for posterior hippocampus).

Reinstatement scores

To identify story-specific and schematic representations at recall, we measured the degree of neural reinstatement of each story during each recall period (**Fig 1D**). Here, we build on prior work on neural reinstatement (e.g., *Xue et al., 2010*; *Staresina et al., 2012*; *Ritchey et al., 2013*; *Wing et al.,*
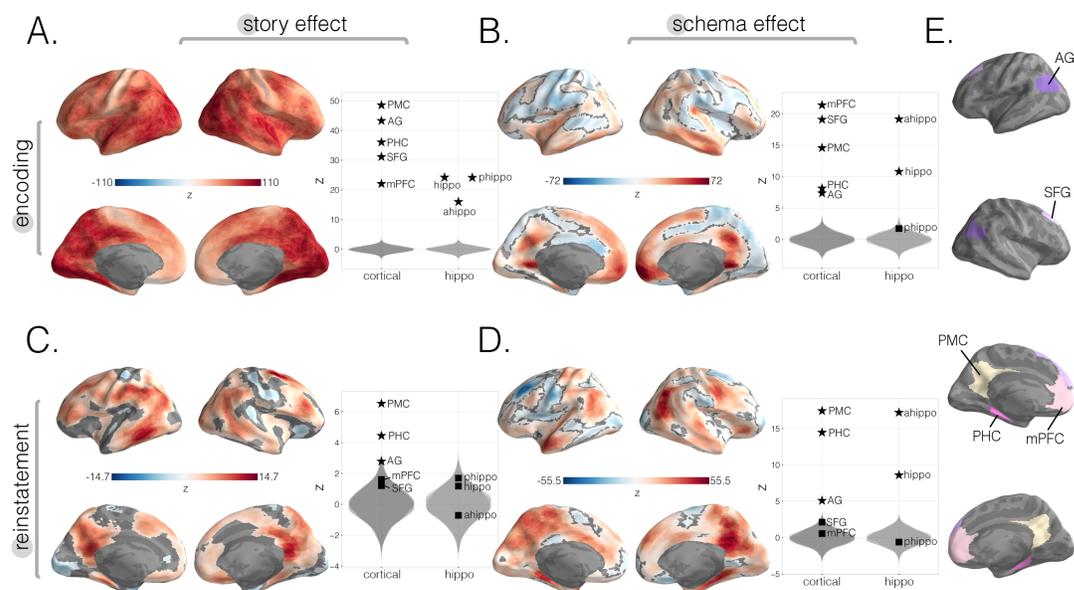
Figure 2. Neural story and schema strength during encoding and retrieval in whole-brain and specific cortical and hippocampal ROIs. (A.) Encoding story scores. **(B.)** Encoding schema scores, **(C.)** Reinstatement story scores. **(D.)** Reinstatement schema scores. All surface maps (**A**, **B**, **C**, and **D**) were colorized with z-scores relative to the null distribution but thresholded via FDR correction for q<0.05 after extracting p-values from a non-parametric permutation test. Plots depict effect sizes in ROIs, z-scored relative to the null distribution (gray). Starred points indicate significant differences after Bonferroni correction for multiple comparisons. **(E.)** Locations of our cortical ROIs.

150 *2015*; *Tompary et al., 2016*; *Chen et al., 2017*) by using a Hidden Markov Model (HMM; *Baldassano*
151 *et al., 2017*) to track reinstatement of sequences of patterns from the encoding phase. We first
152 created "encoding pattern templates" for each of the four events in each story by averaging the
153 evoked response during encoding across all participants experiencing that event. We used these
154 templates to construct 16 different HMMs (one for each story), where the states of each story-
155 specific HMM corresponded to the sequence of four event patterns for that story during encoding.
156 We then applied each of the 16 story-specific HMMs to each recall timeseries, to measure the de-
157 gree to which each story's sequence of patterns was reinstated in that recall timeseries. Essentially,
158 this HMM-fitting process involved – for a given story-specific HMM (from story A) and a given recall
159 timeseries (from story B) – trying to model story B's recall timeseries under the assumption that it
160 contained the same four "template" event patterns (in the same order) as story A. The result of the
161 HMM-fitting process was to subdivide the story B recall timeseries into four contiguous sections
162 that best matched the four encoding-event patterns from story A (see Methods for more details).
163 To measure neural reinstatement, we took the average neural patterns from each of these four
164 sections of the story B recall timeseries, and we correlated these patterns with the actual encoding
165 templates from story A (i.e., we correlated the part of the recall timeseries that the HMM matched
166 to event 1 with the actual encoding pattern for event 1, likewise for events 2, 3, and 4, and then we
167 averaged these four correlations together). By the end of this process, each of the 16 story recalls
168 for a given participant had been compared to each of the 16 story templates from the encoding
169 period. Analogously to the encoding period, we computed – for each participant and each story – a
170 *reinstatement story score* comparing the reinstatement of the matching story to the reinstatement
171 of other stories from the same schema, and a *reinstatement schema score* comparing the reinstate-
172 ment of other studies from the same schema to the reinstatement of other studies from the other
173 schema. These scores were computed in both searchlights and specific ROIs.
174   We found significant reinstatement story scores in regions overlapping with the DMN, partic-

175 ularly lateral posterior SFG, central middle temporal gyrus, PHC, and AG with strongest effects in
176 PMC (**Fig 2C**, q<0.05). Our specific ROI analyses (**Fig 2C**) also showed strong reinstatement story
177 scores in the same regions such as PMC (p<0.01), PHC (p<0.01), AG (p=0.03) but not did not show
178 effects in mPFC (p=0.49), SFG (p > 0.5), nor any of our hippocampal ROIs (full: p>0.5; anterior: p>0.5;
179 posterior: p=0.27). For schema reinstatement, the searchlight analysis revealed positive reinstate-
180 ment schema scores in left anterior temporal pole (AT) as well as a negative effect in areas overlap-
181 ping with left lateral SFG, indicating that stories from the same schema were more differentiated
182 in this region (versus stories from different schemas). Additionally, similar to our encoding results,
183 our specific ROI analyses revealed strong schematic effects in anterior (p<0.01) but not posterior
184 hippocampus (p> 0.5). In contrast to our encoding results, we did not find schema reinstatement
185 effects in mPFC (**Fig 2D**, p>0.5) nor SFG (p=0.15). However, we did find schema reinstatement ef-
186 fects in PMC (p<0.01), PHC (p<0.01), and AG (p<0.01).

187 **Predicting memory performance from story and schema encoding and reinstate-**
188 **ment scores**
189 To identify the degree to which story-specific or schematic neural representations predicted later
190 memory for story details, we ran four separate leave-one-subject-out linear regressions using each
191 of the four neural story and schema scores as single predictor variables (i.e. encoding story, encod-
192 ing schema, reinstatement story and reinstatement schema scores) and memory performance on
193 individual stories (assessed as the number of story-specific details mentioned during free recall)
194 as the outcome variable (**Fig 1E**). Note that the null distributions used to assess the statistical relia-
195 bility of these regression results were constructed by scrambling the relationship between neural
196 data and behavior within subjects (see Methods for more details); as such, significant results in-
197 dicate a reliable *within-subject predictive relationship* between neural measures associated with a
198 story and behavioral recall performance for that story.

199 Memory as a function of encoding story and schema scores
200 Encoding story scores predicted subsequent memory for story details in a very wide range of cor-
201 tical regions (**Fig 3A**, q<0.05). In agreement with the searchlight analysis, we also found signifi-
202 cant positive effects in our cortical and hippocampal ROIs (**Fig 3A**, p<0.01 for all regions, except
203 for p=0.04 for anterior hippocampus). The correlation between encoding story scores and sub-
204 sequent memory was significantly more positive for posterior vs. anterior hippocampus (t(58) =
205 -74.74, p<0.001). We found a sparser set of regions when using encoding schema scores to predict
206 behavior. Based on our searchlight results, the strongest positive effects were found in regions
207 overlapping with the left primary visual cortex, prostriata, anterior mPFC, left posterior temporal
208 sulcus, and left subcentral and postcentral gyrus (**Fig 3B**, q<0.05). Interestingly, we also found re-
209 verse effects (with more schematic information at encoding predicting poorer story-specific mem-
210 ory performance) in multiple regions including bilateral SPL (**Fig 3B**, q<0.05). When we looked for
211 correlations between encoding schema scores and recall behavior in our cortical ROIs, we did not
212 find any strong effects (**Fig 3B**), including our broad mPFC ROI, despite finding a correlation be-
213 tween encoding schema scores and recall behavior in its most anterior portion via the searchlight
214 analysis. Lastly, when we analyzed subsections of the hippocampus, we found opposite correla-
215 tions between encoding schema scores and subsequent memory, with significant negative effects
216 in posterior hippocampus (p<0.01) and numerically positive but non-significant effects in anterior
217 hippocampus (p=0.26). The effects in these two subregions were significantly different from each
218 other when we compared their model coefficients (anterior - posterior) across participants (t(58) =
219 107, p<0.001).

220 Memory as a function of reinstatement story and schema scores
221 Reinstatement story scores were related to recall of specific story details in many regions, with the
222 strongest effects in areas overlapping with bilateral PMC, right mPFC and right anterior temporal
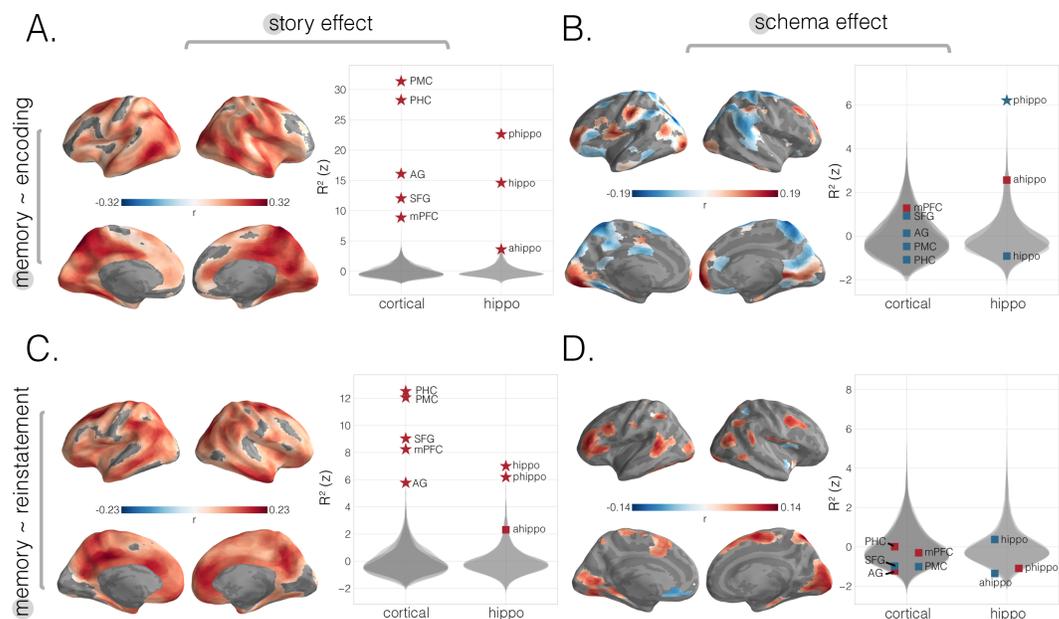
Figure 3. Predicting behavioral memory for story details with neural measures from encoding and recall. We predicted behavioral memory performance on held-out subjects based on each of our 4 neural scores (from **Fig 2**), across the neocortex and in specific ROIs. **(A.)** Predicting memory scores using encoding story scores. **(B.)** Predicting memory scores using encoding schema scores. **(C.)** Predicting memory scores using reinstatement story scores. **(D.)** Predicting memory scores using reinstatement schema scores. All surface maps were statistically thresholded by comparing model performance on held-out data to a null distribution and then FDR correcting for q < 0.05. Surface maps are colored based on the correlation values between neural scores and behavioral memory performance. All violin plots show R^2 values describing model performance z-scored relative to the null distribution. Starred points indicate significant differences after Bonferroni correction for multiple comparisons. Point colors indicate directionality of prediction with red and blue for positive and negative associations, respectively.

Figure 3–Figure supplement 1. Predicting PMC reinstatement story scores with encoding schema scores across cortex

cortex (**Fig 3C**). These effects were also confirmed in our larger cortical ROIs: There were signifi-
cant effects in mPFC, SFG, and AG, and the strongest effects were in PMC and PHC (**Fig 3C**). In our
hippocampus ROIs, we found that reinstatement story scores in posterior and not anterior hip-
pocampus positively predicted subsequent memory (**Fig 3C**); the effect for posterior hippocampus
was significantly larger than the effect for anterior hippocampus (t(58) = -28.48, p<0.001). In the
searchlight analysis with reinstatement schema scores as a predictor variable, the strongest signif-
icant effects were in regions overlapping with bilateral primary visual cortices, bilateral posterior
temporal sulcus, PHC, partial sections of medial SFG, right SPL, and lateral PFC (**Fig 3D**). There were
no significant effects in the *a priori* cortical or hippocampal ROIs (**Fig 3D**). Additionally, because our
PMC ROI was a strong predictor of story-specific behavioral memory and prior work implicates it
in scene-specific representations (*Chen et al., 2017*), we wanted to determine how schematic rep-
resentations across the brain at encoding relate to PMC's story-specific representations at recall
(**Fig 3 Supp 1**). We found that, across the brain, schematic representations in bilateral visual cortex,
angular gyrus, and fusiform cortex were the best predictors of PMC's reinstatement story effect.
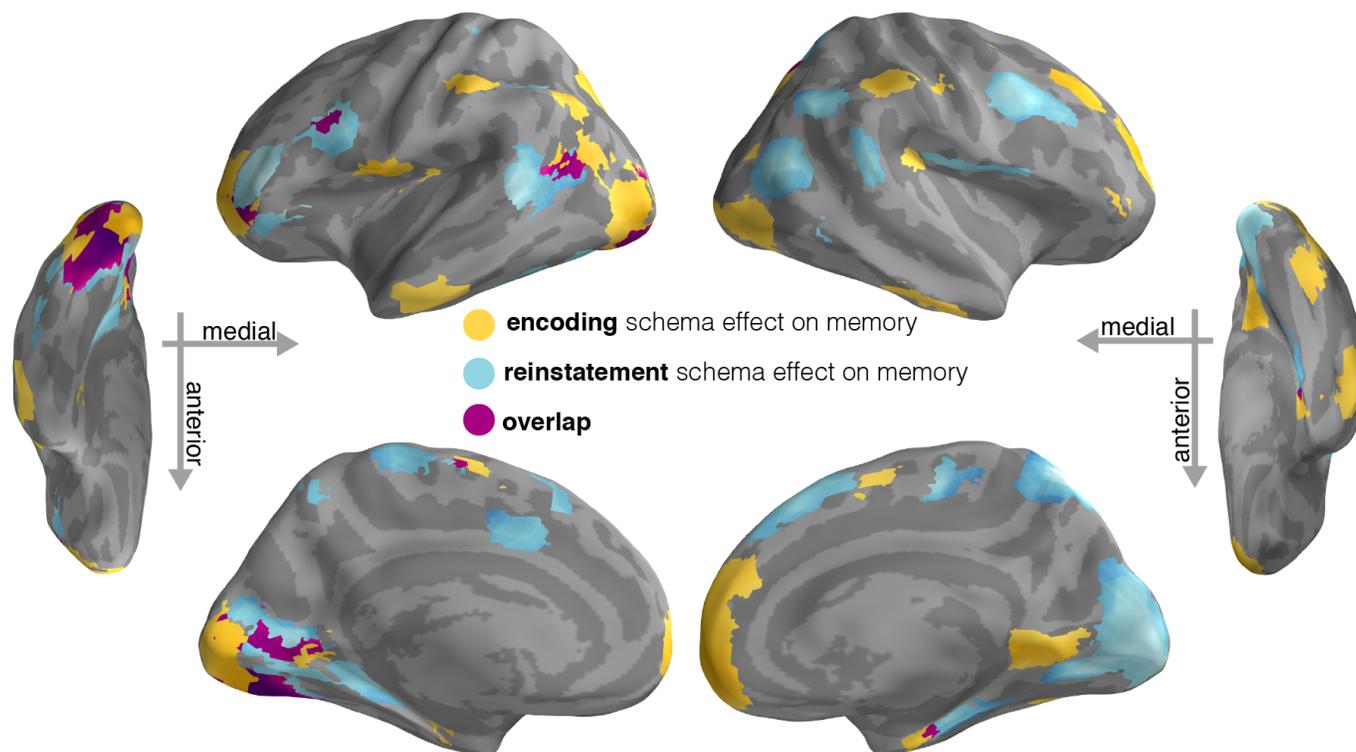
Figure 4. Regions with significant schema effects and positive associations with subsequent memory. To combine the schema and regression effect at encoding, we intersected the regions showing a positive encoding schema effect (**Fig 2B**, q<0.001) with the regions showing a positive relationship between the encoding schema effect and memory behavior (**Fig 3B**, q<0.05); intersection shown in yellow. To combine the schema and regression effect at recall, we intersected the regions showing a positive reinstatement schema effect (**Fig 2D**, q<0.001) with the regions showing a positive relationship between the reinstatement schema effect and memory behavior (**Fig 3D**, q<0.05); intersection shown in light blue. Regions in purple indicate overlap between encoding and retrieval schema networks.

Intersection of significant schema effects and subsequent memory effects

To summarize the key regions in which schematic representations were robustly activated and supported memory performance, we intersected regions of the brain that showed significant schema scores and also showed a positive correlation with later memory for story details. During encoding (**Fig 4A**), this conjunction analysis identified regions in visual cortex, left posterior temporal sulcus, prostriata, entorhinal cortex, left subcentral gyrus, postcentral sulcus, right lateral SFG, and anterior mPFC. For retrieval (**Fig 4B**), we found effects in visual cortex, posterior superior temporal sulcus, left fusiform gyrus, right SPL, right AG, PHC, medial SFG, and middle frontal gyrus.

mPFC clustering and mediation analysis

K-means clustering

Do separate sub-regions within mPFC serve separate functions in memory? Our results indicated that, during perception of schematic information, only the most anterior sections of mPFC showed a correlation between encoding schema scores and subsequent memory for story details (**Fig 3B**). Thus, in order to identify functional differences within mPFC, we ran a k-means clustering analysis. We first pooled the results of our 8 whole-brain searchlight results together (i.e. **Fig 2** and **Fig 3**: story and schema encoding and reinstatement scores as well as their relationships to subsequent memory for story details) to obtain an eight-feature representation for each searchlight location (i.e., the eight features were the eight searchlight values for that location). We then ran a silhou-
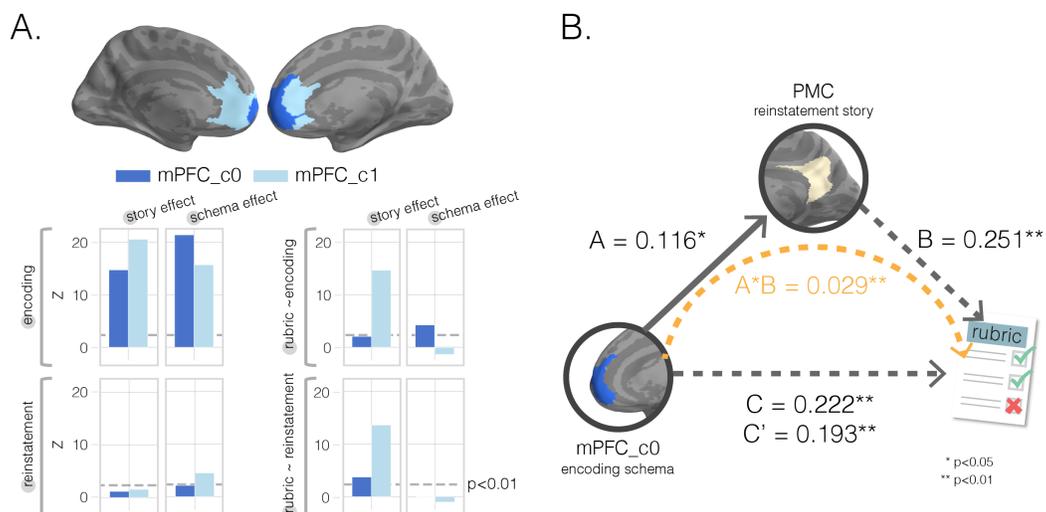
Figure 5. Mediation analysis with mPFC subclusters. (A.) k-means clustering results. We performed post-hoc k-means (k=2) clustering within a bilateral mPFC ROI using our searchlight results (**Fig 2** and **Fig 3**) as features. Encoding schema scores were numerically higher in posterior vs. anterior mPFC (first row). Importantly, in keeping with our searchlight results, encoding schema scores in the most anterior cluster (mPFC_c0, dark blue) were associated with increased memory performance. **(B.)** Mediation analysis. To determine whether PMC story information at recall mediated mPFC's impact on memory accuracy, we ran a single-mediator model with mPFC_c0's encoding schema score as the causal variable, PMC's reinstatement story score as the mediator, and rubric-derived memory scores as our outcome variable. We found that PMC reinstatement story scores were a significant partial mediator.

255 ette analysis on these eight-feature representations to determine the optimal number of clusters
256 to use within a bilateral mPFC ROI mask (restricting the number of clusters k to be less than the
257 number of input features). The analysis revealed that k=2 yielded the highest average silhouette
258 coefficient (s = 0.38). With this k=2 solution, we found that the two clusters separated along the
259 anterior-posterior axis in both hemispheres (**Fig 5A**). We then re-ran our previous analyses (e.g.,
260 encoding story score, encoding schema score, etc.) using these clusters as ROIs to identify (post-
261 hoc) how the properties of these regions differed. We found that both clusters exhibited story and
262 schema effects at encoding, but the contributions of these effects to subsequent memory differed
263 across clusters: The encoding schema effect predicted subsequent memory in the anterior cluster
264 but not the posterior cluster; by contrast, the relationship between the encoding story effect and
265 subsequent memory was much larger in the posterior cluster than the anterior cluster. This flip
266 in subsequent memory contributions between the anterior and posterior mPFC regions is consis-
267 tent with a gradient of story representation to schema representation within mPFC, with schema
268 representations in anterior (vs. posterior) mPFC being most critical for behavior.

269 mPFC cluster mediation

270 Having shown that encoding schema scores in anterior mPFC predict subsequent behavioral recall
271 performance, we sought to relate this effect to the neural reinstatement effects discussed earlier.
272 One hypothesis is that schema information in anterior mPFC at encoding boosts behavioral recall
273 by promoting the (subsequent) neural reinstatement of story-specific information in regions like
274 PMC. To test this hypothesis, we looked at whether the relationship between encoding schema
275 scores in the anterior mPFC cluster and behavioral recall was mediated by PMC story information
276 at recall (**Fig 5B**). Indeed, we found that PMC story information acted as a partial mediator between
277 mPFC_c0 schema information at encoding and later memory (indirect effect A*B = 0.029, 95% bias-
278 corrected bootstrap CI [0.006, 0.057]).

Discussion

In this study, we investigated how our schematic knowledge about the sequential nature of common real-life experiences shapes memory for specific narratives during two distinct phases: when we initially encode a new experience, and when we search our memory to retrieve it. We examined regions in the brain that exhibited schematic patterns at encoding and retrieval and measured the degree to which schematic information in both of these stages predicted subsequent memory for story details. In our prior work using this airport / restaurant paradigm, we had identified a large region of mPFC that represents schema information at encoding. Here, we found that an (anterior) subset of this region had the property that the level of schema representation during encoding predicted subsequent memory for the story (measured using free recall). We also found that, while mPFC played an important role in schema representation during encoding of the stories presented here, it did not reliably represent schema information during recall of these stories, and the degree of schema representation in mPFC during recall did not reliably predict behavior. Consistent with ongoing research on functional differences along the long axis of the hippocampus (for a review see *Poppenk et al., 2013*), we found a major difference in how schema representations in anterior and posterior hippocampus contributed to subsequent memory at encoding. Anterior hippocampus showed a high level of schema representation at encoding and a nonsignificant positive relationship between schema representation at encoding and subsequent memory; in contrast, the level of schema representation in posterior hippocampus at encoding was significantly *negatively* correlated with subsequent memory for the stories. Furthermore, neither hippocampal region showed significant relationships between schema representation and behavior at recall. More generally, the brain regions where schema representation during encoding predicted behavioral memory performance (visual cortex, left posterior temporal sulcus, prostriata, entorhinal cortex, left subcentral gyrus, postcentral sulcus, right lateral SFG, and anterior mPFC) were surprisingly distinct from the brain regions where schema representation during recall predicted behavioral memory performance (bilateral visual regions that were generally more medial/anterior than the regions identified at encoding, posterior superior temporal sulcus, left fusiform gyrus, right SPL, right AG, PHC, medial SFG, and middle frontal gyrus). As a whole, these results provide evidence that event schemas support memory for the details of naturalistic narrative stimuli, and that the brain networks that provide this support are different when we are integrating situational information during perception and when we search for memories during retrieval.

Stimuli and design

The schema literature in fMRI has been mostly split between studies that investigate the role of schemas at encoding and those that investigate their role in retrieval (but see *Bonasia et al., 2018*; *Sommer, 2016*; *van der Linden et al., 2017*; *Raykov et al., 2021*; *Reagh et al., 2021*). Of the studies focusing on the encoding phase, schemas have been operationalized by contrasting conditions in which participants have relevant prior knowledge vs. when they do not have this knowledge (*Maguire et al., 1999*; *van Kesteren et al., 2010a*, *2014*; *Raykov et al., 2018*, *2020*; *Keidel et al., 2018*; *Liu et al., 2017*, *2018*; *Sommer, 2016*) or by using stimuli that are consistent vs. inconsistent with an activated schema (*van Kesteren et al., 2013*, *2020*; *Bonasia et al., 2018*; *van der Linden et al., 2017*). Of the studies focusing on the retrieval phase, schemas have been studied through spatial paired associate tasks (PAs) (*van Buuren et al., 2014*; *Sommer, 2016*; *Guo and Yang, 2020*; *Müller et al., 2020*), learned rules or hierarchies (*Wagner et al., 2015*; *Brod et al., 2015*), simple associations (*van Kesteren et al., 2010b*), static pictures (*Webb et al., 2016*; *Webb and Dennis, 2019*; *van der Linden et al., 2017*), and short video clips (*Bonasia et al., 2018*; *Raykov et al., 2021*; *Reagh et al., 2021*). In contrast to this past work, our design employed naturalistic, temporally-extended schema-consistent stimuli that were then paired with realistic unpaced verbal recall. Importantly, our design allowed us to neurally estimate the degree of story-specific and schematic representation for each individual story, at both encoding and retrieval, across cortex and also in hippocampus; we were able to leverage this to explore how all of these factors related to behavioral memory

329 for story details, in a story-by-story fashion.

Relationship between schematic representations during encoding and subsequent memory

332 As was shown in a previous analysis of this dataset (*Baldassano et al., 2018*), schema representa-
333 tions were present at encoding in many regions previously identified in other studies of schemas,
334 including mPFC (*van Kesteren et al., 2013*, *2014*, *2020*; *Raykov et al., 2020*; *Liu et al., 2017*; *Brod*
335 *and Shing, 2018*; *Sommer, 2016*; *Bonasia et al., 2018*; *Reagh et al., 2021*), PMC (*Maguire et al., 1999*;
336 *van Kesteren et al., 2013*; *Sommer, 2016*; *Bonasia et al., 2018*), SFG (*Bonasia et al., 2018*; *Brod and*
337 *Shing, 2018*), PHC (*Keidel et al., 2018*; *van Kesteren et al., 2014*; *Liu et al., 2017*; *Bonasia et al., 2018*;
338 *van der Linden et al., 2017*), AG (*Keidel et al., 2018*; *Bonasia et al., 2018*; *van der Linden et al., 2017*),
339 and the hippocampus (*van Kesteren et al., 2013*, *2014*; *Raykov et al., 2020*; *Liu et al., 2017*). We also
340 identified strong schema representation in prostriata (*Mikellidou et al., 2017*), a region anterior to
341 V1 and in between RSC and parahippocampal cortex.

342   Since having similar patterns across multiple stories is partially in conflict with having highly
343 distinct story-specific patterns, it is not immediately obvious that maintaining schematic patterns
344 that are shared across stories should be helpful for remembering story-specific information (for
345 evidence of a tradeoff between recall of item-specific vs. shared information, see *Tompary and*
346 *Davachi, 2017*). However, we found multiple regions in which maintenance of this abstract schematic
347 information was associated with improved memory for story details, including anterior mPFC, lat-
348 eral frontal cortex, and portions of visual cortex (**Fig 4A**). Previous studies have shown that greater
349 levels of mPFC activation at encoding are associated with better memory for schema-consistent
350 stimuli (e.g., *Raykov et al., 2021*; *van Kesteren et al., 2013*, *2014*; *Brod and Shing, 2018*); our results
351 extend the literature by revealing a within-subjects (across-story) relationship between the activa-
352 tion of anterior mPFC schema representations at encoding and memory for details of temporally-
353 extended naturalistic stimuli. Surprisingly, we also found that schema representations in visual
354 cortex contribute to memory. It is possible that certain visual features (e.g., visual features of secu-
355 rity lines for airports, or tables for restaurants) are central to the mental representations of these
356 airport and restaurant schemas; as such, increased attention to these visual features (for movies)
357 and/or visualization of these features (for audio narratives) may reflect stronger schema represen-
358 tation, leading to improved memory encoding.

359   In the hippocampus, we found diverging effects in posterior and anterior subregions, with
360 schematic patterns at encoding being nonsignificantly helpful for memory in anterior hippocam-
361 pus but significantly harmful to memory in posterior hippocampus (the difference between these
362 effects was also significant). Furthermore, while both posterior and anterior hippocampus exhib-
363 ited significant story-specific representation at encoding, the correlation between encoding story
364 scores and subsequent memory was significantly larger for posterior hippocampus. Taken to-
365 gether, these results suggest that posterior hippocampus plays an especially important role in
366 representing story-specific details, consistent with theories of gist vs. detail representations in the
367 hippocampus (*Guo and Yang, 2020*; *Audrain and McAndrews, 2020*; *Poppenk et al., 2013*; *Brunec*
368 *et al., 2018*; *Schlichting et al., 2015*; *Collin et al., 2015*; *Sekeres et al., 2018*; for data suggesting a
369 reversed gradient see *Tompary and Davachi, 2017*; *Dandolo and Schwabe, 2018*).

Relationship between schematic representations during retrieval and memory performance

372 We identified a set of regions in which schematic codes were reactivated during retrieval, and the
373 degree of reactivation was related to behavioral recall performance. These regions were largely
374 non-overlapping with those from the encoding-phase analysis, and included fusiform gyrus, middle
375 frontal gyrus, and posterior parietal regions including right angular gyrus and SPL. Left fusiform
376 gyrus and AG have been associated with visual imagery (*Spagna et al., 2021*; *Ragni et al., 2020*;
377 *Kuhl and Chun, 2014*), and posterior parietal regions such as SPL have been implicated in top-down

378 attention during episodic memory retrieval (*Hutchinson et al., 2014*; *Wagner et al., 2005*; *Cabeza*
379 *et al., 2008*) and general memory success (*Brod et al., 2015*; *Webb et al., 2016*). Because no visual
380 cue (apart from the title of a story) was provided during recall, participants may need to rely on
381 top-down generation of visual cues to orient to particular schema stages (e.g., generating a mental
382 image of what airport security usually looks like, to cue memory for the airport security part of an
383 airport narrative).

384   Many of the regions listed above (posterior parietal regions as well as lateral temporal cortex,
385 superior frontal gyrus, middle frontal gyrus, and visual regions) have previously been implicated in
386 schematic memory (*Guo and Yang, 2020*; *Webb and Dennis, 2019*; *Brod et al., 2015*; *van der Linden*
387 *et al., 2017*), but they have also been reported to be involved in memory even when there is no
388 schema manipulation (*van Buuren et al., 2014*; *van Kesteren et al., 2010b*, *2020*; *Webb et al., 2016*;
389 *Webb and Dennis, 2019*; *Brod et al., 2015*). Since our study can separately measure both story-
390 specific and schematic reactivation patterns during naturalistic recall, we were able to show that
391 there was a memory boost from schema-related reactivation in these regions in addition to more
392 general story reactivation effects.

393   Given the strong involvement of mPFC during schematic encoding, it has been hypothesized
394 that mPFC may play a role at retrieval by providing schematic cues for memory search (*van Kesteren*
395 *et al., 2012*). While some studies have found that schema-related activity in mPFC during retrieval
396 benefits memory (*Brod et al., 2015*; *van Kesteren et al., 2010b*; *Müller et al., 2020*; *Webb and Den-*
397 *nis, 2019*; *Raykov et al., 2021*), others have not (*van Buuren et al., 2014*; *Webb et al., 2016*; *Guo*
398 *and Yang, 2020*; *van der Linden et al., 2017*; *Reagh et al., 2021*). In our study, we did not observe
399 strong mPFC schema reinstatement, nor were able to relate it to a behavioral memory benefit. It is
400 possible that schema representations in mPFC contribute to retrieval, but we failed to detect this
401 contribution, e.g., because they only emerge at specific time points during recall, or they only arise
402 after sleep consolidation (*van der Linden et al., 2017*; *Brod et al., 2015*; *van Kesteren et al., 2010b*),
403 or they contribute through interactions with other brain regions (*Guo and Yang, 2020*; *van Kesteren*
404 *et al., 2010b*). Alternatively, schematic representations in mPFC during recall may be associated
405 less with accurate recall of specific story details and more with verbal descriptions of schematic
406 elements of the narrative. Because the rubric we made for scoring memory performance tracks
407 recall of story-specific details, it is not ideal for measuring the extent to which a recall conforms to
408 the general (restaurant or airport) schema. Future work exploring the relationship between neural
409 measures and verbal recall of schematic features could further deepen our understanding of the
410 correspondence between the brain and behavior.

Conclusion

412 In our study, we derived neural measures of story-specific and schematic representations in the
413 brain during the perception and recall of narratives conforming to naturalistic event schemas. Our
414 results extend the literature on the benefits of schemas for memory performance, relating the
415 maintenance of schematic representations to a continuous behavioral measure of detailed mem-
416 ory for realistic narrative stimuli. We found converging support for the idea that schema represen-
417 tations in mPFC play an important role in memory encoding, but also striking differences between
418 regions where schema representation at encoding was useful for memory, and regions where
419 schema representation at retrieval was useful for memory. These findings can serve as a founda-
420 tion for future work that seeks to further delineate the contributions of these encoding-specific
421 and retrieval-specific schema networks.

Methods and materials

Participants

424 Data were collected from a total of 31 participants between the ages of 18-34 (15 female, 16 male).
425 The perception (movie-watching and story-listening) data from these participants have been pre-

426 viously reported (*Baldassano et al., 2018*). At the end of the study, participants were paid and
427 debriefed about the purpose of the study. Every effort was made to recruit an equal number of
428 female and male participants and to ensure that minorities were represented in proportion to the
429 composition of the local community. The experimental protocol was approved by the Institutional
430 Review Board (IRB) of Princeton University and all participants provided their written informed
431 consent. Due to data loss during the recall phase, one participant (female) was excluded from the
432 recall analyses.

Stimuli

434 The stimuli were designed to conform to two naturalistic schematic scripts that participants had
435 encountered throughout their lifetimes. Each of the 16 stories described the schematic script of
436 either eating at a restaurant or catching a flight at an airport (*Bower et al., 1979*). Each narrative
437 was written or edited to follow a specific 4-stage event structure. For restaurant stories, the event
438 structure consisted of 1) entering and being taken to a table, 2) sitting with menus, 3) ordering food
439 and waiting for its arrival, and 4) food arriving and being eaten; while airport narratives consisted
440 of 1) entering the airport, 2) going through the security, 3) walking to and waiting at the gate, and
441 4) getting onboard the plane and sitting in a seat.

442 The videos were movie clips sampled from films (restaurant: Brazil, Derek, Mr. Bean, Pulp
443 Fiction; airport: Due Date, Good luck Chuck, Knight and Day, Non-stop) that were edited for length
444 and to conform to the 4-stage script. The audio stimuli were adapted from film scripts (restaurant:
445 The Big Bang Theory, The Santa Clause, Shame, My Cousin Vinny; airport: Friends, How I met Your
446 Mother, Seinfeld, Up in the Air) that were also edited for length and to match the schematic script.
447 All audio narratives were read by the same professional actor. Each story, whether video or audio,
448 was approximately 3 minutes long.

Data acquisition and preprocessing

450 Data were acquired with a voxel size of 2.0mm isotropic and a TR of 1.5 s (see *Baldassano et al.,*
451 *2018* for a full description of the sequence parameters). After fMRI data were aligned and prepro-
452 cessed to correct for B0 distortion and fsaverage6 resampling, the resampled data were further
453 preprocessed with a custom Python script that first removed nuisance regressors (the 6 degrees
454 of freedom motion correction estimates, and low-order Legendre drift polynomials up to order [1
455 + duration/150] as in Analysis of Functional NeuroImages [AFNI]) (*Cox, 1996*), then z-scored each
456 run, and then divided the runs into the portions corresponding to each stimulus (see *Baldassano*
457 *et al., 2018* for a more detailed description of our preprocessing pipeline).

Experimental paradigm

459 After listening to a short unrelated audio clip to verify that the volume level was set correctly, partic-
460 ipants were presented with four encoding runs, using PsychoPy (RRID:SCR_006571; *Peirce, 2007*).
461 Each run consisted of interleaved video and audio stories, with one story from each modality and
462 schema in each run, and a randomized run order across subjects. Every story was preceded by a
463 5 s black screen followed by a 5 s countdown video. The title of each story was displayed at the
464 top of the screen throughout the story (the screen was otherwise black for the audio narratives).
465 participants were informed that they would be asked to freely recall the stories after all 16 had
466 been presented.

467 During the recall phase, participants were asked to freely verbally recall (at their own pace) the
468 details of each story when cued by the title of the story-to-remember. When participants finished
469 recalling a particular story, they said "Done" to signal the experimenter for the next title. There
470 were four recall runs in total. During each recall run, participants were cued to recall four sto-
471 ries, with a 1 minute rest between each story recall. After recalling all 16 stories, while still being
472 scanned, participants were asked to provide verbal descriptions of the typical experience of eating
473 at a restaurant and the typical experience of going through an airport.

Searchlights and ROIs

Searchlights

Our searchlights were generated by randomly sampling a center vertex of the fsaverage6 surface mesh and identifying all vertices within 11 steps from it. Because the vertex spacing within the fsaverage6 mesh is 1.4 mm, the resulting radius is 15 mm. Searchlights were repeatedly sampled (discarding searchlights containing fewer than 100 vertices with valid timeseries) until every center vertex was included in at least 10 searchlights. This process yielded 1483 searchlights per hemisphere.

A priori ROIs

Following recent work on the encoding of narrative event schemas using the same encoding dataset (*Baldassano et al., 2018*), as well as prior research on the representation of high level situation models (*Zadbood et al., 2017*; *Chen et al., 2017*; *Baldassano et al., 2017*; *Kurby and Zacks, 2008*; *Radvansky and Zacks, 2017*; *Nguyen et al., 2019*; *Clewett et al., 2019*), we focused our main ROI analyses on medial prefrontal cortex (mPFC), posterior medial cortex (PMC), superior frontal gyrus (SFG), angular gyrus (AG), and parahippocampal cortex (PHC) because of their consistent presence in naturalistic paradigms and their role in maintaining schema representations during encoding. The regions were extracted from an established 17-network atlas on the fsaverage6 surface (*Yeo et al., 2011*) that formed part of the larger default mode network. Our full hippocampus ROI was extracted from a freesurfer subcortical parcellation, which was then further split between an anterior at y > -20 and posterior portion at y <= -20 in MNI space (*Guo and Yang, 2020*; *Poppenk et al., 2013*).

Measuring story and schema strength in verbal and neural data

Encoding similarity matrix

For each story, we created four regressors to model the neural response to each of the four schematic events (i.e., the four stages of the script), with an additional nuisance regressor to model the initial countdown. The four regressors (and nuisance regressor) in our design matrix were placed temporally by using hand-labeled timestamps that marked event-transitions in the narratives. These were convolved with an HRF from AFNI (*Cox, 1996*) and then z-scored. We extracted the characteristic spatial pattern across vertices for each schematic event within a story by fitting a GLM (within each participant) to the timeseries of each vertex using these regressors. Next, to quantify the degree to which stories evoked similar neural patterns, we used intersubject spatial pattern similarity (e.g., *Raykov et al., 2020*; *Baldassano et al., 2018*; *Chen et al., 2017*) – specifically, the event-specific patterns for a given story / participant were always compared to patterns that were derived from the N-1 other participants (by averaging the timecourses for the N-1 other participants for a given story, and then fitting a GLM to that averaged timecourse to identify the four event-specific patterns for that story). To compute the similarity for a given pair of stories (call them A and B) , the pattern vectors for each of story A's four events were correlated with the pattern vectors for each of story B's four events (i.e., the event 1 pattern for story A was correlated with the event 1 pattern for story B from the N-1 other participants; the event 2 pattern for story A was correlated with the event 2 pattern for story B from the N-1 other participants, and so on). These four correlation values for a given pair of stories (event 1 to event 1, event 2 to event 2, etc.) were averaged into a single value. For each participant, this sequence of steps was used to compare that participant's representation of each story to the N-1 other participants' representation of each story. The net result of this process was a 16x16 correlation (similarity) matrix for every participant, containing the (intersubject) neural similarity of each story to every other story (see **Fig 1C**).

Reinstatement similarity matrix

First, we created a template for each of the four events in each story, by using a GLM to extract the multivoxel BOLD pattern for that event within each participant, and then averaging across participants to get a single spatial pattern for that event (**Fig 1D**). We then sought to measure the extent to which these story-specific patterns were reinstated during the free recall period with the Hidden Markov Model (HMM) approach used in *Baldassano et al.* (*2017*, 2018). The model makes the assumption that, when recalling a story, the event pattern templates from encoding are replayed in the same ordered sequence. The variance parameter for the model was calculated per participant by measuring the variance of that story's mean event patterns at perception. Given a template pattern for a story (i.e. its 4-stage encoding pattern), and the timeseries for the recall of that story, the model computes a probability that each time point of the recall belongs to each of the 4 template events. We then computed a weighted average spatial pattern for each event during the recall, using the probability matrix as the weights. To determine the strength of reinstatement between the template story and the recalled story, each of the four encoding event template patterns was correlated with all of the four recall event patterns, the strength of reinstatement was measured as the difference between the correlations for corresponding (e.g. encoding template event 1 and recall event 1) and non-corresponding events (e.g. encoding template event 1 and recall event 2). This difference measure per event was averaged and was repeated for all combinations of template story and recall story, yielding a 16x16 encoding-recall similarity matrix per participant (see **Fig 1D**). Importantly, while our HMM method is biased to recover patterns that match the encoding templates, this bias applies equally regardless of which stories are being compared; our reinstatement story and schema measures control for this bias by looking at the *relative* degree of reinstatement across different comparisons (e.g., comparing reinstatement of stories from the same schema vs. stories from the other schema).

Story and schema scores

Because we generated both an encoding and reinstatement similarity matrix for every participant, we could then perform contrasts for each stimulus for each participant (during encoding or recall) to measure the extent to which neural representations contain story-specific or schematic information.

Story score (**Fig 1C, 1D**): To compute the *story score* for a particular story, we contrasted that story's similarity to itself (a square on the diagonal of the similarity matrix) with the average of that story's similarity to other stories from the same schema and modality (the modality restriction was done to avoid effects driven by overall modality differences unrelated to this particular story). We determined statistical significance for the difference in similarity using a non-parametric permutation test in which we randomly permuted the stories within a schema 1000 times to generate a null distribution of differences. A p value was computed as the proportion of times a difference in the null distribution was greater than or equal to the difference of the correctly labeled data.

Schema score (**Fig 1C, 1D**): To compute the *schema score* for a particular story, we contrasted the average of that story's similarity to other stories from the same schema with the average of that story's similarity to other stories from the other schema (using only stories from the same modality). Statistical significance was determined in a non-parametric permutation test in which schema labels of stories were randomly permuted 1000 times.

To generate brainmaps of these scores, story and schema information were extracted from the encoding and reinstatement similarity matrices computed at each searchlight (**Fig 1**). To convert searchlights back to the cortical surface, the score for each vertex was computed as the average scores of all searchlights that included that vertex. Similarly, we averaged the null distributions for all searchlights that included a vertex to get a single null distribution per vertex. P-values were obtained per vertex through a two-sided nonparametric permutation test that looked for the proportion of times an absolute value in the null distribution (created by shuffling story labels separately for each participant) was greater than the absolute value of the original averaged story or schema

570 score. We then converted these p-values to q-values using the false discovery rate correction from
571 AFNI (*Cox, 1996*).

Behavior

Verbal recall analysis (rubrics; **Fig 1E**): Hand-scored rubrics were used to provide a quantita-
tive behavioral measure of memory recall performance for details within a story (available here).
Rubrics for videos included points for recalling unchanging ("static") details (e.g. character appear-
ance, set design) and "dynamic" details (e.g., combined dialogue and visual descriptions). For audio
stories, only "dynamic" details were tracked (given the lack of visual information). Transcripts for
audio stories were split into sentences and points were awarded if a detail from at least a fraction
of a sentence was recalled. Participant audio was recorded during free recalls and was manually
timestamped, transcribed and scored for memory performance using the rubrics. Memory per-
formance was measured by the number of details remembered (sum of points) and normalized
by total possible details for a given story (as measured by max possible rubric score for a story).
Two independent coders scored every participant's memory performance (intercoder reliability,
pearson r = .95) and final scores per story were averaged across both independent coders.

Predicting behavioral performance from neural scores

We next wanted to identify whether the story and schema scores at encoding or recall predicted
behavioral memory performance. In other words, how does the neural representation of story
and schema information at either encoding or recall predict later memory?

To answer this question, we conducted four separate leave-one-participant-out linear regres-
sion analyses for each ROI or searchlight. Each of the four regression analyses used a particu-
lar neural score (either encoding story, encoding schema, reinstatement story or reinstatement
schema) to predict behavioral recall performance, on a story-by-story basis. The regression mod-
els were trained on neural scores and behavioral scores from all but one participant; we then used
the trained model to predict the left-out participant's 16 behavioral recall scores (one per story;
Fig 1F) based on that participant's neural scores. Each of the four regressions was run with each
of the 30 subjects as a test subject, providing a 30x16 matrix of behavioral predictions on held-out
subjects. With these predictions, model performance was measured by variance explained (R^2)
compared to a baseline model of simply predicting the average rubric score of the N-1 group. Sta-
tistical significance was determined through nonparametric permutation testing, in which a null
distribution of 1,000 values was made by shuffling the story scores within each subject (thereby
keeping the subjects intact) before running the leave-one-out regression. To visualize searchlight
results on the cortical surface, we averaged R^2 scores across searchlights in the same way that was
described above for the story and schema scores (i.e., each vertex was assigned the average R^2
across all of the searchlights that included that vertex).

With simple linear regression, predictions of rubric scores below zero were possible, despite
zero being the lowest possible rubric score. To enforce realistic predictions of rubric scores of
greater or equal to zero, we also ran the same regression procedure with a logistic output layer;
the results of this analysis were highly similar to the results that we obtained when we used linear
regression. Consequently, for the sake of simplicity, we only describe the results for simple linear
regression here.

ROI to ROI correlations

Because story information was most strongly reinstated in PMC (**Fig 2**), and this reinstatement was
highly predictive of behavioral rubric scores (**Fig 3**), we examined whether there were neural sig-
nals during encoding that were predictive of later PMC story reinstatement. To do this, we ran a
linear regression with PMC's reinstatement story score as the dependent variable and each search-
light's encoding schema score as the independent measure. To test for significance, we generated
a null distribution in which story labels for the dependent variable were shuffled within subjects.

618 In this nonparametric permutation 2-sided test, p-values were computed by calculating the pro-
619 portion of absolute values above the test-value. Searchlights were converted back to vertex-space
620 before converting the p-values to q-values with AFNI's FDR-correction. To visualize the results on
621 a brainmap, vertices were thresholded at q<0.05.

Schema representation and subsequent behavior

623 To identify regions where schema information was represented and the degree of that schema
624 representation influenced memory, we intersected positive schema effects (thresholded by FDR <
625 0.001; **Fig 3B**) with regions that were positively correlated with later memory (thresholded by FDR
626 < 0.05; **Fig 3D**, right column). We did this for encoding (**Fig 4A**) and recall (**Fig 4B**) separately.

K-means clustering and mediation analysis

628 Although the full mPFC ROI showed strong schema representation during perception (**Fig 2**), the
629 behavioral prediction searchlights revealed that schema information only predicted behavior in
630 the most anterior portion of mPFC (**Fig 3B**). To explore the differential functional roles of mPFC
631 subregions, we ran a post-hoc K-means clustering analysis to segment our mPFC ROI into 2 clusters
632 with distinct functional profiles (**Fig 5**). Using the results of 8 different searchlights (**Fig 2** and **Fig 3**)
633 as features, we generated clusters across multiple k's bilaterally on searchlight vertices using our *a*
634 *priori* mPFC ROI as a mask. We first ran a silhouette analysis to determine the optimal k (restricting
635 k to be less than the number of input features); then, for each resulting cluster, we calculated new
636 similarity matrices, extracted story and schema scores, and ran our behavioral prediction analysis
637 (**Fig 5**).
638 We also ran an additional mediation analysis to identify the extent to which PMC and mPFC sub-
639 regions interacted to support recall (**Fig 5B**). Our goal was to determine whether the behavioral im-
640 pact of schematic representations in mPFC at encoding was mediated through the reinstatement
641 of story information in PMC. To do this, we ran a traditional single-mediator model in which the
642 causal, mediator and outcome variables were mPFC subregion schema information at encoding,
643 PMC story information at recall, and rubric scores, respectively (*Baron and Kenny, 1986*). The total
644 effect of the causal variable mPFC schema at encoding on the outcome rubric scores (path c) was
645 calculated by running a linear regression with each regressor standardized. The significance of
646 the effect was computed by generating a null distribution from shuffling the labels of the outcome
647 variable, generating a corresponding z-value for the original effect, and converting to a p-value
648 from the survival function of the normal distribution. This same procedure was used to test for
649 the significance of each individual component in the indirect effect (paths a and b) as well as the
650 direct effect (path c'). To test for statistical significance of the indirect effect (i.e. mediated effect),
651 we performed a bias-corrected bootstrap test (*Efron and Tibshirani, 1994*). To determine the speci-
652 ficity of this effect, we also ran a variant of this analysis where swapped the roles of the two ROIs,
653 using the PMC encoding schema score as the causal variable and mPFC subregion reinstatement
654 story score as the mediator. We found no significant effects in this analysis.

References

663 **Abbott V**, Black JB, Smith EE. The representation of scripts in memory. Journal of Memory and Language. 1985
664 4; 24(2):179–199. doi: 10.1016/0749-596X(85)90023-3.

665 **Alba JW**, Hasher L. Is memory schematic? Psychological Bulletin. 1983; 93(2):203–231. doi: 10.1037//0033-
666   2909.93.2.203.

667 **Anderson RC**, Pichert JW. Recall of previously unrecallable information following a shift in perspective. Journal
668   of Verbal Learning and Verbal Behavior. 1978 2; 17(1):1–12. doi: 10.1016/S0022-5371(78)90485-1.

669 **Audrain S**, McAndrews MP. Schemas provide a scaffold for neocortical integration at the cost of memory
670   specificity over time; 2020, https://doi.org/10.1101/2020.10.11.335166, doi: 10.1101/2020.10.11.335166.

671 **Baldassano C**, Chen J, Zadbood A, Pillow JW, Hasson U, Norman KA. Discovering event structure in continu-
672   ous narrative perception and memory. Neuron. 2017 8; 95(3):709–721. https://pubmed.ncbi.nlm.nih.gov/
673   28772125/, doi: 10.1016/j.neuron.2017.06.041.

674 **Baldassano C**, Hasson U, Norman KA. Representation of real-world event schemas during narrative perception.
675   Journal of Neuroscience. 2018 11; 38(45):9689–9699. https://doi.org/10.1523/JNEUROSCI.0251-18.2018, doi:
676   10.1523/JNEUROSCI.0251-18.2018.

677 **Baron RM**, Kenny DA. The moderator-mediator variable distinction in social psychological research: Concep-
678   tual, strategic, and statistical considerations. Journal of Personality and Social Psychology. 1986; 51(6):1173–
679   1182. doi: 10.1037//0022-3514.51.6.1173.

680 **Bein O**, Reggev N, Maril A. Prior knowledge influences on hippocampus and medial prefrontal
681   cortex interactions in subsequent memory. Neuropsychologia. 2014 11; 64:320–330. doi:
682   10.1016/j.neuropsychologia.2014.09.046.

683 **Bonasia K**, Sekeres MJ, Gilboa A, Grady CL, Winocur G, Moscovitch M. Prior knowledge modulates the
684   neural substrates of encoding and retrieving naturalistic events at short and long delays. Neurobiol-
685   ogy of Learning and Memory. 2018 9; 153(Pt A):26–39. https://pubmed.ncbi.nlm.nih.gov/29474955/, doi:
686   10.1016/j.nlm.2018.02.017.

687 **Bower GH**, Black JB, Turner TJ. Scripts in memory for text. Cognitive Psychology. 1979 4; 11(2):177–220. doi:
688   10.1016/0010-0285(79)90009-4.

689 **Bransford JD**, Johnson MK. Contextual prerequisites for understanding: some investigations of comprehen-
690   sion and recall. Journal of Verbal Learning and Verbal Behavior. 1972 12; 11(6):717–726. doi: 10.1016/S0022-
691   5371(72)80006-9.

692 **Brewer WF**, Nakamura GV. The nature and functions of schemas. Champaign, Ill: University of Illinois at
693   Urbana-Champaign; 1984.

694 **Brod G**, Lindenberger U, Werkle-Bergner M, Shing YL. Differences in the neural signature of remembering
695   schema-congruent and schema-incongruent events. NeuroImage. 2015 8; 117:358–366. https://pubmed.
696   ncbi.nlm.nih.gov/26048620/, doi: 10.1016/j.neuroimage.2015.05.086.

697 **Brod G**, Shing YL. Specifying the role of the ventromedial prefrontal cortex in memory for-
698   mation. Neuropsychologia. 2018 3; 111:8–15. https://pubmed.ncbi.nlm.nih.gov/29317324/, doi:
699   10.1016/j.neuropsychologia.2018.01.005.

700 **Brunec IK**, Bellana B, Ozubko JD, Man V, Robin J, Liu ZX, Grady C, Rosenbaum RS, Winocur G, Barense
701   MD, Moscovitch M. Multiple scales of representation along the hippocampal anteroposterior axis in
702   humans. Current Biology. 2018 7; 28(13):2129–2135. https://pubmed.ncbi.nlm.nih.gov/29937352/, doi:
703   10.1016/j.cub.2018.05.016.

704 **van Buuren M**, Kroes MCW, Wagner IC, Genzel L, Morris RGM, Fernández G. Initial investigation of the effects
705   of an experimentally learned schema on spatial associative memory in humans. Journal of Neuroscience.
706   2014 12; 34(50):16662–16670. doi: 10.1523/JNEUROSCI.2365-14.2014.

707 **Cabeza R**, Ciaramelli E, Olson IR, Moscovitch M. The parietal cortex and episodic memory: An attentional
708   account. Nature Reviews Neuroscience. 2008 8; 9(8):613–625. https://pubmed.ncbi.nlm.nih.gov/18641668/,
709   doi: 10.1038/nrn2459.

710 **Chen J**, Leong YC, Honey CJ, Yong CH, Norman KA, Hasson U. Shared memories reveal shared structure in
711   neural activity across individuals. Nature Neuroscience. 2017 1; 20(1):115–125. https://www.nature.com/
712   articles/nn.4450, doi: 10.1038/nn.4450.

713 **Clewett D**, DuBrow S, Davachi L. Transcending time in the brain: How event memories are constructed
714 from experience. Hippocampus. 2019 3; 29(3):162–183. https://pubmed.ncbi.nlm.nih.gov/30734391/, doi:
715 10.1002/hipo.23074.

716 **Collin SHP**, Milivojevic B, Doeller CF. Memory hierarchies map onto the hippocampal long axis in hu-
717 mans. Nature Neuroscience. 2015 11; 18(11):1562–1564. https://pubmed.ncbi.nlm.nih.gov/26479587/, doi:
718 10.1038/nn.4138.

719 **Cox RW**. AFNI: Software for analysis and visualization of functional magnetic resonance neuroimages. Com-
720 puters and Biomedical Research. 1996; 29(3):162–173. https://pubmed.ncbi.nlm.nih.gov/8812068/, doi:
721 10.1006/cbmr.1996.0014.

722 **Dandolo LC**, Schwabe L. Time-dependent memory transformation along the hippocampal anterior-posterior
723 axis. Nature Communications. 2018 12; 9(1):1–11. doi: 10.1038/s41467-018-03661-7.

724 **Efron B**, Tibshirani RJ. An Introduction to the Bootstrap - 1st Edition - Bradley Efron - R.J. 1 ed. Boca Raton:
725 Chapman and Hall/CRC; 1994.

726 **Ghosh VE**, Gilboa A. What is a memory schema? A historical perspective on current neuroscience literature.
727 Neuropsychologia. 2014 1; 53(1):104–114. doi: 10.1016/j.neuropsychologia.2013.11.010.

728 **Gilboa A**, Marlatte H. Neurobiology of schemas and schema-mediated memory. Trends in Cognitive Sciences.
729 2017 8; 21(8):618–631. https://pubmed.ncbi.nlm.nih.gov/28551107/, doi: 10.1016/j.tics.2017.04.013.

730 **Graesser AC**, Nakamura GV. The impact of a schema on comprehension and memory. Psychology of Learning
731 and Motivation - Advances in Research and Theory. 1982 1; 16(C):59–109. doi: 10.1016/S0079-7421(08)60547-
732 2.

733 **Guo D**, Yang J. Interplay of the long axis of the hippocampus and ventromedial prefrontal cortex in schema-
734 related memory retrieval. Hippocampus. 2020 3; 30(3):263–277. https://pubmed.ncbi.nlm.nih.gov/31490611/,
735 doi: 10.1002/hipo.23154.

736 **Hutchinson JB**, Uncapher MR, Weiner KS, Bressler DW, Silver MA, Preston AR, Wagner AD. Functional hetero-
737 geneity in posterior parietal cortex across attention and episodic memory retrieval. Cerebral Cortex. 2014
738 1; 24(1):49–66. https://pubmed.ncbi.nlm.nih.gov/23019246/, doi: 10.1093/cercor/bhs278.

739 **Keidel JL**, Oedekoven CSH, Tut AC, Bird CM. Multiscale integration of contextual information during a natu-
740 ralistic task. Cerebral Cortex. 2018 10; 28(10):3531–3539. https://pubmed.ncbi.nlm.nih.gov/28968727/, doi:
741 10.1093/cercor/bhx218.

742 **van Kesteren MTR**, Rijpkema M, Ruiter DJ, Morris RGM, Fernández G. Building on prior knowledge:
743 schema-dependent encoding processes relate to academic performance. Journal of Cognitive Neuro-
744 science. 2014 10; 26(10):2250–2261. http://www.mitpressjournals.org/doi/10.1162/jocn_a_00630, doi:
745 10.1162/jocn{_}a{_}00630.

746 **van Kesteren MTR**, Krabbendam L, Meeter M. Integrating educational knowledge: reactivation of prior knowl-
747 edge during educational learning enhances memory integration. npj Science of Learning. 2018 12; 3(1):11.
748 doi: 10.1038/s41539-018-0027-8.

749 **van Kesteren MTR**, Beul SF, Takashima A, Henson RN, Ruiter DJ, Fernández G. Differential roles for medial
750 prefrontal and medial temporal cortices in schema-dependent encoding: From congruent to incongruent.
751 Neuropsychologia. 2013 10; 51(12):2352–2359. doi: 10.1016/j.neuropsychologia.2013.05.027.

752 **van Kesteren MTR**, Fernández G, Norris DG, Hermans EJ. Persistent schema-dependent hippocampal-
753 neocortical connectivity during memory encoding and postencoding rest in humans. Proceedings of the
754 National Academy of Sciences of the United States of America. 2010 4; 107(16):7550–7555. https://www.
755 pnas.org/content/107/16/7550, doi: 10.1073/pnas.0914892107.

756 **van Kesteren MTR**, Rignanese P, Gianferrara PG, Krabbendam L, Meeter M. Congruency and reactivation
757 aid memory integration through reinstatement of prior knowledge. Scientific Reports. 2020 12; 10(1):1–13.
758 https://doi.org/10.1038/s41598-020-61737-1, doi: 10.1038/s41598-020-61737-1.

759 **van Kesteren MTR**, Rijpkema M, Ruiter DJ, Fernández G. Retrieval of associative information congruent with
760 prior knowledge is related to increased medial prefrontal activity and connectivity. Journal of Neuroscience.
761 2010 11; 30(47):15888–15894. https://pubmed.ncbi.nlm.nih.gov/21106827/, doi: 10.1523/JNEUROSCI.2674-
762 10.2010.

763 **van Kesteren MTR**, Ruiter DJ, Fernández G, Henson RN. How schema and novelty augment memory for-
764 mation. Trends in Neurosciences. 2012 4; 35(4):211–219. https://pubmed.ncbi.nlm.nih.gov/22398180/, doi:
765 10.1016/j.tins.2012.02.001.

766 **Kuhl BA**, Chun MM. Successful remembering elicits event-specific activity patterns in lateral parietal cor-
767 tex. Journal of Neuroscience. 2014; 34(23):8051–8060. https://pubmed.ncbi.nlm.nih.gov/24899726/, doi:
768 10.1523/JNEUROSCI.4328-13.2014.

769 **Kurby CA**, Zacks JM. Segmentation in the perception and memory of events. Trends in Cognitive Sciences.
770 2008 2; 12(2):72–79. https://pubmed.ncbi.nlm.nih.gov/18178125/, doi: 10.1016/j.tics.2007.11.004.

771 **van der Linden M**, Berkers RMWJ, Morris RGM, Fernández G. Angular gyrus involvement at encoding and
772 retrieval is associated with durable but less specific memories. Journal of Neuroscience. 2017 9; 37(39):9474–
773 9485. https://pubmed.ncbi.nlm.nih.gov/28871031/, doi: 10.1523/JNEUROSCI.3603-16.2017.

774 **Liu ZX**, Grady C, Moscovitch M. Effects of prior-knowledge on brain activation and connectivity during as-
775 sociative memory encoding. Cerebral Cortex. 2017 3; 27(3):1991–2009. https://pubmed.ncbi.nlm.nih.gov/
776 26941384/, doi: 10.1093/cercor/bhw047.

777 **Liu ZX**, Grady C, Moscovitch M. The effect of prior knowledge on post-encoding brain connectivity and its
778 relation to subsequent memory. NeuroImage. 2018 2; 167:211–223. doi: 10.1016/j.neuroimage.2017.11.032.

779 **Maguire EA**, Frith CD, Morris RGM. The functional neuroanatomy of comprehension and memory: the impor-
780 tance of prior knowledge. Brain. 1999 10; 122(10):1839–1850. https://academic.oup.com/brain/article-lookup/
781 doi/10.1093/brain/122.10.1839, doi: 10.1093/brain/122.10.1839.

782 **Mandler JM**. Stories, scripts, and scenes: Aspects of schema theory. 1 ed. New York: Psychology Press; 2014.
783 doi: 10.4324/9781315802459.

784 **McAndrews MP**, Girard TA, Wilkins LK, McCormick C. Semantic congruence affects hippocam-
785 pal response to repetition of visual associations. Neuropsychologia. 2016 9; 90:235–242. doi:
786 10.1016/j.neuropsychologia.2016.07.026.

787 **McClelland JL**, McNaughton BL, Lampinen AK. Integration of new information in memory: New insights from
788 a complementary learning systems perspective. Philosophical Transactions of the Royal Society B: Biological
789 Sciences. 2020 5; 375(1799). doi: 10.1098/rstb.2019.0637.

790 **Mikellidou K**, Kurzawski JW, Frijia F, Montanaro D, Greco V, Burr DC, Morrone MC. Area prostriata in the human
791 brain. Current Biology. 2017 10; 27(19):3056–3060. doi: 10.1016/j.cub.2017.08.065.

792 **Müller NCJ**, Dresler M, Janzen G, Beckmann CF, Fernández G, Kohn N. Medial prefrontal decou-
793 pling from the default mode network benefits memory. NeuroImage. 2020 4; 210:116543. doi:
794 10.1016/j.neuroimage.2020.116543.

795 **Nguyen M**, Vanderwal T, Hasson U. Shared understanding of narratives is correlated with shared neu-
796 ral responses. NeuroImage. 2019 1; 184:161–170. https://pubmed.ncbi.nlm.nih.gov/30217543/, doi:
797 10.1016/j.neuroimage.2018.09.010.

798 **Peirce JW**. PsychoPy-Psychophysics software in Python. Journal of Neuroscience Methods. 2007 5; 162(1-2):8–
799 13. https://pubmed.ncbi.nlm.nih.gov/17254636/, doi: 10.1016/j.jneumeth.2006.11.017.

800 **Poppenk J**, Evensmoen HR, Moscovitch M, Nadel L. Long-axis specialization of the human hippocampus.
801 Trends in Cognitive Sciences. 2013 5; 17(5):230–240. https://pubmed.ncbi.nlm.nih.gov/23597720/, doi:
802 10.1016/j.tics.2013.03.005.

803 **Preston AR**, Eichenbaum H. Interplay of hippocampus and prefrontal cortex in memory. Current Biology. 2013
804 9; 23(17):R764–R773. https://pubmed.ncbi.nlm.nih.gov/24028960/, doi: 10.1016/j.cub.2013.05.041.

805 **Radvansky GA**, Zacks JM. Event boundaries in memory and cognition. Current Opinion in Behavioral Sciences.
806 2017 10; 17:133–140. doi: 10.1016/j.cobeha.2017.08.006.

807 **Ragni F**, Tucciarelli R, Andersson P, Lingnau A. Decoding stimulus identity in occipital, parietal and inferotem-
808 poral cortices during visual mental imagery. Cortex. 2020 6; 127:371–387. https://pubmed.ncbi.nlm.nih.gov/
809 32289581/, doi: 10.1016/j.cortex.2020.02.020.

810 **Raykov PP**, Keidel JL, Oakhill J, Bird CM. Shared contextual knowledge strengthens inter-subject synchrony and
811 pattern similarity in the semantic network; 2018, https://doi.org/10.1101/276683, doi: 10.1101/276683.

Raykov PP, Keidel JL, Oakhill J, Bird CM. The brain regions supporting schema-related processing of people's identities. Cognitive Neuropsychology. 2020 2; 37(1-2):8–24. https://www.tandfonline.com/doi/full/10.1080/02643294.2019.1685958, doi: 10.1080/02643294.2019.1685958.

Raykov PP, Keidel JL, Oakhill J, Bird CM. Activation of Person Knowledge in Medial Prefrontal Cortex during the Encoding of New Lifelike Events. Cerebral Cortex. 2021 4; 00:1–12. https://academic.oup.com/cercor/advance-article/doi/10.1093/cercor/bhab027/6236062, doi: 10.1093/cercor/bhab027.

Reagh ZM, Ranganath C, Louis S. A cortico-hippocampal scaffold for representing and recalling lifelike events; 2021, https://doi.org/10.1101/2021.04.16.439894, doi: 10.1101/2021.04.16.439894.

Ritchey M, Wing EA, LaBar KS, Cabeza R. Neural similarity between encoding and retrieval is related to memory via hippocampal interactions. Cerebral cortex (New York, NY : 1991). 2013 12; 23(12):2818–2828. doi: 10.1093/cercor/bhs258.

Schank RC, Abelson RP. Scripts, plans and knowledge. In: *Proceedings of the Fourth International Joint Conference on Artificial Intelligence*; 1975. p. 151–157.

Schlichting ML, Mumford JA, Preston AR. Learning-related representational changes reveal dissociable integration and separation signatures in the hippocampus and prefrontal cortex. Nature Communications. 2015 8; 6(1):1–10. doi: 10.1038/ncomms9151.

Schlichting ML, Preston AR. Memory integration: Neural mechanisms and implications for behavior. Current Opinion in Behavioral Sciences. 2015 2; 1:1–8. https://pubmed.ncbi.nlm.nih.gov/25750931/, doi: 10.1016/j.cobeha.2014.07.005.

Schlichting ML, Preston AR. Hippocampal–medial prefrontal circuit supports memory updating during learning and post-encoding rest. Neurobiology of Learning and Memory. 2016 10; 134(Part A):91–106. doi: 10.1016/j.nlm.2015.11.005.

Sekeres MJ, Winocur G, Moscovitch M. The hippocampus and related neocortical structures in memory transformation. Neuroscience Letters. 2018 7; 680:39–53. doi: 10.1016/j.neulet.2018.05.006.

Sommer T. The emergence of knowledge and how it supports the memory for novel related information. Cerebral Cortex. 2016 2; 27(3):1906–1921. http://cercor.oxfordjournals.org/cgi/doi/10.1093/cercor/bhw031, doi: 10.1093/cercor/bhw031.

Spagna A, Hajhajate D, Liu J, Bartolomeo P. Visual mental imagery engages the left fusiform gyrus, but not the early visual cortex: A meta-analysis of neuroimaging evidence. Neuroscience and Biobehavioral Reviews. 2021 3; 122:201–217. doi: 10.1016/j.neubiorev.2020.12.029.

Spalding KN, Jones SH, Duff MC, Tranel D, Warren DE. Investigating the neural correlates of schemas: Ventromedial prefrontal cortex is necessary for normal schematic influence on memory. Journal of Neuroscience. 2015 11; 35(47):15746–15751. https://www.jneurosci.org/content/35/47/15746https://www.jneurosci.org/content/35/47/15746.abstract, doi: 10.1523/JNEUROSCI.2767-15.2015.

Staresina BP, Henson RNA, Kriegeskorte N, Alink A. Episodic reinstatement in the medial temporal lobe. Journal of Neuroscience. 2012 12; 32(50):18150–18156. http://www.fil.ion.ucl.ac.uk/spm/, doi: 10.1523/JNEUROSCI.4156-12.2012.

Tompary A, Davachi L. Consolidation promotes the emergence of representational overlap in the hippocampus and medial prefrontal cortex. Neuron. 2017 9; 96(1):228–241. doi: 10.1016/j.neuron.2017.09.005.

Tompary A, Duncan K, Davachi L. High-resolution investigation of memory-specific reinstatement in the hippocampus and perirhinal cortex. Hippocampus. 2016 8; 26(8):995–1007. https://onlinelibrary.wiley.com/doi/full/10.1002/hipo.22582https://onlinelibrary.wiley.com/doi/abs/10.1002/hipo.22582https://onlinelibrary.wiley.com/doi/10.1002/hipo.22582, doi: 10.1002/hipo.22582.

Tompary A, Thompson-Schill SL. Semantic influences on episodic memory distortions. Journal of Experimental Psychology: General. 2021 1; /record/2021-07872-001, doi: 10.1037/xge0001017.

Tse D, Langston RF, Kakeyama M, Bethus I, Spooner PA, Wood ER, Witter MP, Morris RGM. Schemas and memory consolidation. Science. 2007 4; 316(5821):76–82. www.sciencemag.org/cgi/content/full/316/5821/73/DC1, doi: 10.1126/science.1135935.

Tse D, Takeuchi T, Kakeyama M, Kajii Y, Okuno H, Tohyama C, Bito H, Morris RGM. Schema-dependent gene activation and memory encoding in neocortex. Science. 2011 8; 333(6044):891–895. https://pubmed.ncbi.nlm.nih.gov/21737703/, doi: 10.1126/science.1205274.

Wagner AD, Shannon BJ, Kahn I, Buckner RL. Parietal lobe contributions to episodic memory retrieval. Trends in Cognitive Sciences. 2005 9; 9(9):445–453. https://pubmed.ncbi.nlm.nih.gov/16054861/, doi: 10.1016/j.tics.2005.07.001.

Wagner IC, van Buuren M, Kroes MC, Gutteling TP, van der Linden M, Morris RG, Fernández G. Schematic memory components converge within angular gyrus during retrieval. eLife. 2015 11; 4. doi: 10.7554/elife.09668.

Wang SH, Morris RGM. Hippocampal-neocortical interactions in memory formation, consolidation, and reconsolidation. Annual Review of Psychology. 2010 1; 61:49–79. https://pubmed.ncbi.nlm.nih.gov/19575620/, doi: 10.1146/annurev.psych.093008.100523.

Webb CE, Dennis NA. Differentiating true and false schematic memories in older adults. Journals of Gerontology - Series B Psychological Sciences and Social Sciences. 2019 9; 74(7):1111–1120. doi: 10.1093/geronb/gby011.

Webb CE, Turney IC, Dennis NA. What's the gist? The influence of schemas on the neural correlates underlying true and false memories. Neuropsychologia. 2016 12; 93(Pt A):61–75. https://pubmed.ncbi.nlm.nih.gov/27697593/, doi: 10.1016/j.neuropsychologia.2016.09.023.

Wing EA, Ritchey M, Cabeza R. Reinstatement of individual past events revealed by the similarity of distributed activation patterns during encoding and retrieval. Journal of Cognitive Neuroscience. 2015 4; 27(4):679–691. http://direct.mit.edu/jocn/article-pdf/27/4/679/1782648/jocn_a_00740.pdf, doi: 10.1162/jocn{_}a{_}00740.

Xue G, Dong Q, Chen C, Lu Z, Mumford JA, Poldrack RA. Greater neural pattern similarity across repetitions is associated with better memory. Science. 2010 10; 330(6000):97–101. doi: 10.1126/science.1193125.

Yeo BT, Krienen FM, Sepulcre J, Sabuncu MR, Lashkari D, Hollinshead M, Roffman JL, Smoller JW, Zöllei L, Polimeni JR, Fisch B, Liu H, Buckner RL. The organization of the human cerebral cortex estimated by intrinsic functional connectivity. Journal of Neurophysiology. 2011 9; 106(3):1125–1165. https://pubmed.ncbi.nlm.nih.gov/21653723/, doi: 10.1152/jn.00338.2011.

Zadbood A, Chen J, Leong YC, Norman KA, Hasson U. How we transmit memories to other brains: constructing shared neural representations via communication. Cerebral Cortex. 2017 10; 27(10):4988–5000. https://pubmed.ncbi.nlm.nih.gov/28922834/, doi: 10.1093/cercor/bhx202.
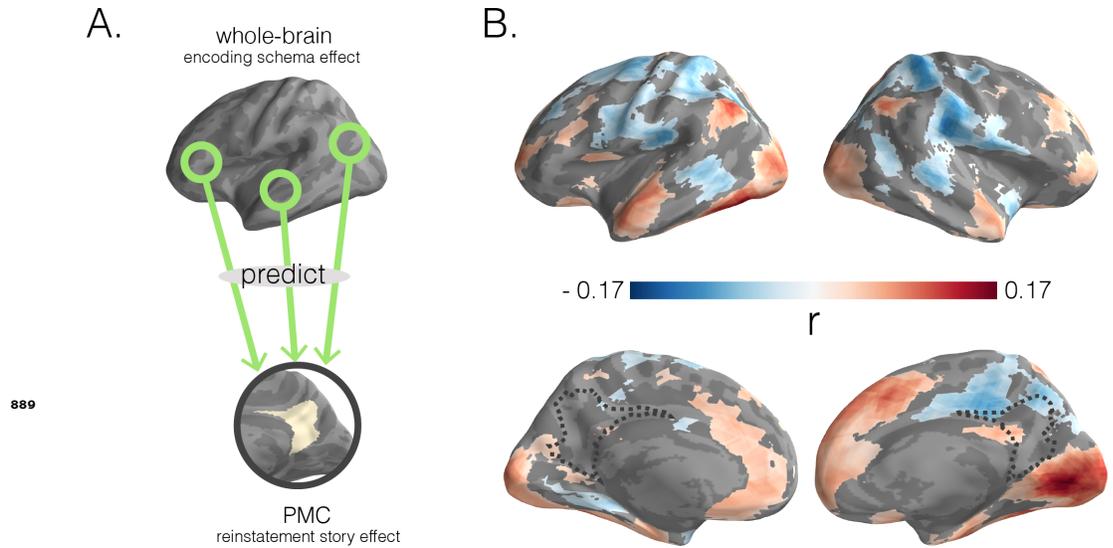
Figure 3–Figure supplement 1. Predicting PMC reinstatement story scores with encoding schema scores across cortex. (A.) In a searchlight analysis, we used encoding schema scores across the brain to predict reinstatement story scores in PMC. **(B.)** Dark blue to dark red gradients represent negative to positive strength of associations between encoding schema scores (for the colored region) and PMC reinstatement story scores. Surface maps were statistically thresholded by comparing model performance on held-out data to a null distribution and then FDR correcting for q < 0.05.